

doi: 10.13241/j.cnki.pmb.2018.13.009

Micro-CT 监测尼古丁对大鼠正畸牙移动过程中牙周改建的影响 *

孙鲁旻¹ 杨东红¹ 王凯² 房玉镇³ 韩兆国² 叶之慧^{1△}

(1 佳木斯大学附属口腔医院正畸科 黑龙江 佳木斯 154004;

2 哈尔滨医科大学附属第四医院分子影像研究中心 黑龙江 哈尔滨 150000;3 济南市第三人民医院口腔科 山东 济南 250000)

摘要 目的:探讨不同摄取量的尼古丁对大鼠正畸过程牙周改建的影响。**方法:**选择 120 只雄性 Wistar 大鼠并将其随机分为四组: A 组 - 空白对照, B 组 - 正畸模型, C 组 - 正畸并 0.01 mg/mL 尼古丁给药, D 组 - 正畸并 1 mg/mL 尼古丁给药。分别于实验开始后第 1、3、7、14、21 天通过 Micro-CT 和 HE 染色观察模型牙齿移动距离和牙周组织改变并通过 ELISA 实验检测 IL-17 的表达。**结果:**Micro-CT 扫描显示:正畸建模组相对于空白对照组在牙移动距离、骨体积分数、骨密度等指标均有明显变化,变化最大幅度发生在 D 组,B、C 两组之间的差异没有统计学意义($P>0.05$)。21 天,D 组移动距离达到 0.80 ± 0.06 mm,明显高于 B、C 组($P<0.05$)。相较于空白对照组(A 组),B、C、D 三组 Micro-CT 测量的骨体积分数、骨密度、骨小梁厚度均降低,D 组骨密度值降至 1108.36 ± 8.86 mg/cm³。HE 染色结果显示:D 组在 21 天时破骨细胞增多并出现牙根吸收陷窝伴牙周膜纤维排列混乱;ELISA 检测显示 B、C 组 IL-17 的含量在第 7 天时达到峰值,D 组则在 14 天含量最高。**结论:**高浓度的尼古丁可加速正畸牙齿的移动速度及牙槽骨吸收,增加牙周组织中的破骨细胞及 IL-17 表达水平。

关键词:尼古丁;正畸;Micro-CT;骨小梁;IL-17**中图分类号:**R-33; R783.5 **文献标识码:**A **文章编号:**1673-6273(2018)13-2448-04

Effect of Nicotine on the Periodontium during Orthodontic Tooth Movement in Rats Monitored by Micro-CT*

SUN Lu-min¹, YANG Dong-hong¹, WANG Kai², FANG Yu-zhen³, HAN Zhao-guo², YE Zhi-hui^{1△}

(1 Department of Orthodontic, Stomatological Hospital Affiliated to Jiamusi University, Jiamusi, Heilongjiang, 154004, China;

2 Molecular Imaging Research Center, The fourth affiliated hospital of Harbin medical university, Harbin, Heilongjiang, 150000, China;

3 Department of Orthodontic, Ji'nan Third People's Hospital, Ji'nan, Shandong, 250000, China)

ABSTRACT Objective: The study the effect of differentdosis of nicotine on the periodontium during orthodontic treatment in adult rats. **Methods:** 120 cases of Wistar male rats were segmented into four groups stochastically: A-control; B-orthodontic model group; C-orthodontic + 0.01 mg/kg nicotine group; D-orthodontic+1 mg/kg nicotine group. Micro-CT was used to measure tooth movement and the changes on microstructure of trabecular, the variety of periodontal microstructures and expression of IL-17 on day 1, 3, 7, 14 and 21 were detected and compared. **Results:** Micro-CT scanning showed that the orthodontic groups changed largely on observed indicators, such as tooth movement, BVF, and BMD, when compared to control groups. There were no significant changes between B and C groups ($P>0.05$), D group changed mostly. The tooth movement of D group reached 0.80 ± 0.06 mm, which was obviously higher than B and C groups at day 21 ($P<0.05$). The BVF, BMD and Tb.Th in all groups lessened apart from A group. HE staining of A - D groups indicated that the ligament of D group was disordering and more osteoclasts. The expression level of IL-17 reached its peak at day 7 in B, C groups, but it was at day 14 for D group. **Conclusion:** High-dose nicotine can not only accelerate the speed of tooth movement and the absorption of alveolar bone;in addition, but also increase the quantity of osteoclast and IL-17 expression.

Key words: Nicotine; Orthodontic; Micro-CT; Trabecular bone; IL-17**Chinese Library Classification(CLC):** R-33; R783.5 **Document code:** A**Article ID:** 1673-6273(2018)13-2448-04

前言

成人正畸治疗已占牙齿矫治总数的 15%~20%,临幊上吸烟的成年患者并不少见^[1]。尼古丁作为烟草的主要成分,易通过口腔粘膜被机体吸收,长期接触会损害牙周组织引起骨丧失

^[2,3]。另外,吸烟可以导致口腔炎症,增加白细胞介素 17(IL-17, interleukin -17)的表达水平,IL-17 又可直接促进破骨细胞形成,而破骨细胞是牙槽骨动态平衡的重要介质^[4-6]。以往对牙周骨改建情况的评价指标多为骨量或组织病理改变,但有研究证实骨小梁的显微结构是判断骨重建的一个重要指标^[7]。微型计算机

* 基金项目:黑龙江省教育厅基础研究项目(2016-KYYWF-0611)

作者简介:孙鲁旻(1989-),硕士研究生,研究方向:口腔正畸学,E-mail: 993237362@qq.com

△ 通讯作者:叶之慧,副教授,硕士生导师,研究方向:口腔正畸学,E-mail: 79033864@qq.com,电话:0454-8625516

(收稿日期:2018-03-05 接受日期:2018-03-28)

断层成像(Micro computed tomography, Micro CT)基于 X 线成像原理可在不破坏样本的情况下对牙槽骨进行三维扫描, 同时对结构、密度等指标进行定量分析^[8-10]。本实验将不同浓度尼古丁涂抹于大鼠口腔, 并通过 Micro-CT 等监测骨小梁的显微结构指标变化, 探讨正畸过程中尼古丁对牙周组织改建的影响, 旨在为吸烟者接受更科学有效的正畸治疗提供理论依据。

1 材料与方法

1.1 主要试剂和仪器

尼古丁溶液(上海抚生实业有限公司);0.9%生理盐水;10%水合氯醛溶液;多聚甲醛;EDTA;HE 染色试剂及电子显微镜;IL-17 酶联免疫吸附实验(ELISA)试剂盒(上海研生实业有限公司), iMark 酶标仪(Bio-Rad 公司, 美国);Micro-CT(Super Argus, Spanish)。

1.2 方法

1.2.1 正畸模型建立和给药方式 雄性 Wistar 大鼠 120 只(3 月龄, 350~400 g) 随机分四组:A 空白组,B 正畸组,C 正畸并 0.01 mg/kg 尼古丁给药组,D 正畸并 1 mg/kg 尼古丁给药组。大鼠以 10% 水合氯醛(0.3 mL/100 g)腹腔注射麻醉后, 仰卧位用慢速金刚砂车针于上颌两中切牙龈缘及左上第一磨牙近中颈缘处预备一深约 0.3 mm 的沟用于固位, 两牙之间用正畸拉簧牵拉, 0.2 mm 结扎丝固定于沟处, 力值约 30 g^[11]。口腔涂抹给药, 每天 2 次, 间隔 6 h, 正畸组同频次涂抹生理盐水。

1.2.2 标本采集 各时间点分别于每组随机选取 6 只大鼠处死, 随机选取 3 只剥取左侧上颌第一磨牙压力侧牙龈组织, 编号后放入 -20 ℃ 冰箱保存待用, 另外 3 只分离左上颌骨, 浸入 4% 多聚甲醛固定液, 24 h 后进行 Micro-CT 扫描, 完成后放入 10% EDTA 脱钙液, 室温脱钙。

1.2.3 Micro-CT 扫描及视图分析 将上颌骨牙冠平行地面固定在扫描床上, 用以下参数扫描:最高分辨率(Max Res), 静态调强模式(step & shot), 720°, 50 KV, 300 μA, 39 ms, 扫描用时约 20 min。图像重建采用配套 Sedecal RECON 软件, 视图分析采用配套 MMWKS 软件及 ImageJ 软件。CT 图上第一磨牙远中和第二磨牙近中的距离即为牙移动距离(mm)。选择左上颌第一磨牙远中颊根根中 1/3 的近中牙槽间隔骨松质为感兴趣区(region of interest, ROI), 三维重建后对骨小梁的显微结构进行定量分析, 包括:骨密度(BMD, mg/cm³)、骨体积分数(BVF, 指 ROI 内的骨小梁体积与所选 ROI 体积比值)、骨小梁厚度(Tb.Th, mm)^[12-14]。

1.2.4 HE 染色 上颌骨标本脱钙 45 天, OCT 包埋后 -80 ℃ 冷冻 1 h, 于冰冻切片机内复温(OT -20 °C, CT -20 °C)1 h 切片, 厚度 5 μm。将切片依次进行苏木素染色、分化、伊红染色、透明化、封片操作, 在 × 400 电子显微镜下观察。

1.2.5 ELISA 实验 将冰箱内牙龈组织取出复温, 加入盛有 0.5 mL 二甲基甲酰胺(DMF)的研磨杵, 制作组织匀浆, 高速离心(1500 rpm, 15 min)。取上清液 100 μL, 按照大鼠 IL-17 ELISA 检测试剂盒标准步骤进行操作, 将样品按 1:2 倍稀释, 最后用酶标仪在 450 nm 波长依序测量各孔的 OD(平均光密度)值, 根据标准品 OD 值和浓度描绘标准曲线, 将样品 OD 值代入标准曲线公式得到对应浓度, 乘稀释倍数 2 则为该样本检测浓度。

1.3 统计学分析

采用 GraphPad Prism 5 统计软件处理。所有数据均以 $\bar{x} \pm s$ 表示($n \geq 3$), 多组间比较采用方差分析, 两组间比较采用 t 检验, 以 $P < 0.05$ 为差异具有统计学意义。

2 结果

2.1 Micro-CT 扫描测量结果

2.1.1 牙移动距离 在实验开始后 1~21 天时间点, A 组在基线范围内变化 ($0.08 \pm 0.01 \sim 0.12 \pm 0.03$), B、C、D 三组的移动距离随时间而增加, 并且 14 天后增速有所放缓, 分别于 21 天达到最大值(B: 0.4 ± 0.07 , C: 0.45 ± 0.045 , D: 0.80 ± 0.06), 其中 14 天、21 天 D 组移动距离高于 B、C 两组具有统计学意义 ($P < 0.05$), 表明高剂量尼古丁局部作用可以促进正畸牙移动。牙移动 CT 检测距离见图 1(a、b、c、d), 具体数值变化趋势见图 3a。

2.1.2 大鼠牙槽骨 Micro-CT 图像及显微结构的骨参数分析 21 天矢状位 CT 图像显示:A 组牙槽骨骨质紧密;B、C 组牙齿移动距离略有增加, 骨质密度有所降低;D 组移动距离最为明显, 骨质密度降低显著, 见图 1。其余骨小梁细微结构的具体指标变化趋势见图 3(a、b) 及图 4(a、b), A 组各指标的变化范围不明显, B、C、D 三组由于加力等原因导致各项指标均有变化, 其中 B、C 之间的微小差距没有统计学意义($P > 0.05$)。D 组变化最为明显, 7 天、14 天、21 天的 BMD、BVF、Tb.Th 均低于 B、C 两组($P < 0.05$), 差异有统计学意义。

2.2 HE 染色结果

A 组牙周膜间隙等宽, 胶原纤维排列规则, 无破骨细胞出现;B 组和 C 组牙周膜变窄, 牙根及牙槽骨边缘粗糙, 周围可见少量破骨细胞, D 组牙周膜明显缩窄, 周围有较多的成熟多核破骨细胞聚集, 牙根可见吸收陷窝。如图 2(a、b、c、d)。

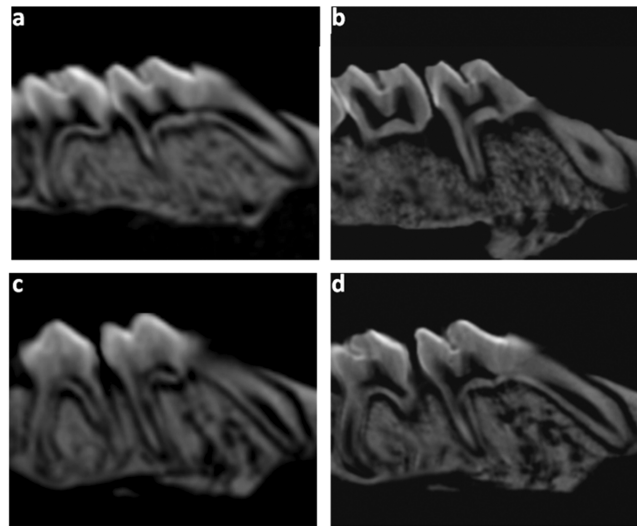


图 1 各组 21 天标本矢状位高分辨率 Micro-CT 图像

Fig.1 The sagittal and high resolution Micro-CT images in each group on Day 21. (a-A Group, b-B Group, c-C Group, d-D Group)

2.3 牙龈组织 IL-17 的表达

ELISA 检测结果显示:各组均有 IL-17 表达, 其中 A 组为正常生理水平, 且基本维持稳定, B、C、D 三组均有先升高后降低的趋势;B、C 组表达水平基本一致, 并于第 7 天达到峰值, 其

后下降;D组在第14天时达到最高表达水平,且明显高于BC两组($P<0.01$),见表1。

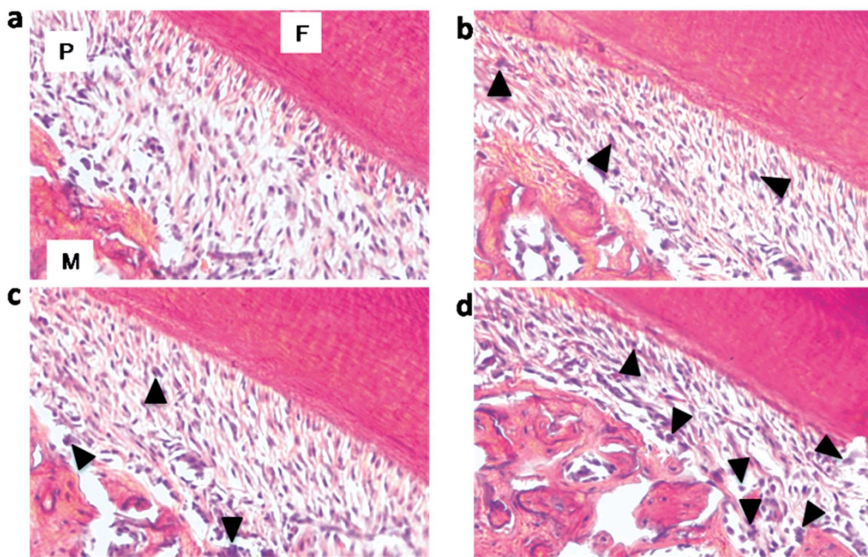


图2 21天各组牙齿标本的HE染色图像

Fig.2 The HE staining of samples in each group at Day 21. (M-alveolar bone, F-tooth root, P-parodontium, Black arrow- osteoclast; a-A Group, b-B Group, c-C Group, d-D Group)

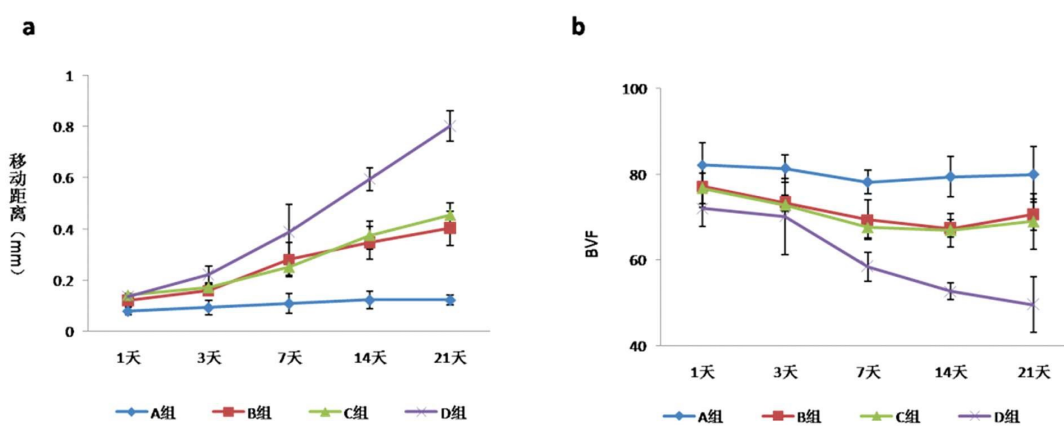


图3 牙齿移动距离和骨体积分数的Micro-CT测量指标变化

Fig.3 The changes of measurement index of Micro-CT for tooth movement and BVF

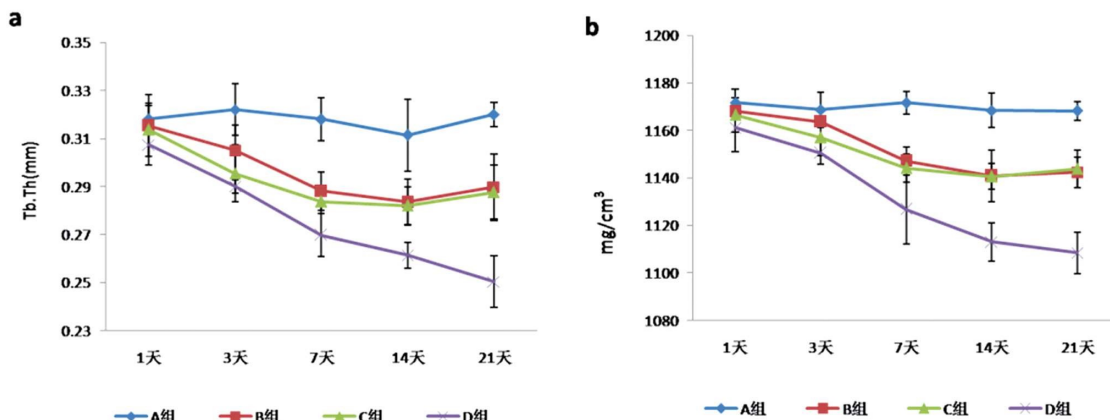


图4 骨小梁厚度和骨密度的Micro-CT测量指标变化

Fig.4 The changes of measurement index of Micro-CT for Tb.Th and BMD

3 讨论

正畸治疗的生物学基础是牙周组织改建,压力侧牙槽骨吸收,张力侧新骨生成,最终使牙齿达到理想位置^[15]。尼古丁可对

表 1 各组大鼠不同时间点 IL-17 的表达水平(单位:pg/mL)($\bar{x}\pm s$, n=3)

Table 1 Expression of IL-17 at different time points of rats in each group($\bar{x}\pm s$, n=3)

Groups	Day 1	Day 3	Day 7	Day 14	Day 21
A Group	22.871± 1.047	22.077± 2.653	24.670± 2.655	21.794± 4.081	24.454± 0.925
B Group	23.415± 2.471	27.552± 3.542	37.915± 5.300	36.812± 4.588	29.502± 6.160
C Group	24.089± 4.005	30.212± 3.977	40.668± 7.025	37.070± 4.175	33.440± 5.1784 6.050± 2.935*
D Group	20.463± 1.680	33.235± 3.824	50.969± 4.521	53.904± 2.357*	46.050± 2.935*

Note: compared with the B and C group at the day 14, *P<0.01; at the day 21, *P<0.05.

骨质改建产生不利影响,吸烟人群牙周附着丧失率约为未吸烟人群的3~4倍,表明尼古丁是加重牙周损伤的危险因素之一^[2]。Mizrak S、Esfahrood ZR等学者通过尼古丁腹腔注射的方法研究其对正畸牙移动的影响,证实尼古丁可以通过血液循环进入到牙周组织来影响正畸过程^[16,17]。本实验采用口腔涂抹的给药方式,更能模拟真实吸烟环境。此外,本实验采用新型影像技术 Micro-CT 对牙周改建各项指标进行检测,可精准测量牙齿移动距离,并可对骨质显微结构进行重建、定量分析^[18,19]。

本研究结果显示正畸模型组由于加力因素破骨细胞数量、牙槽骨显微结构指标、IL-17 水平均较正常对照出现明显变化;正畸模型组和低浓度尼古丁处理正畸模型组变化基本一致,说明低浓度尼古丁正畸过程中牙槽骨改建没有明显影响;高浓度尼古丁处理正畸模型组破骨细胞数量、牙槽骨显微结构指标的变化幅度、IL-17 水平均较任何一组更为明显,而且压力侧的牙根表面出现吸收陷窝。另外,根据牙槽骨显微结构指标的变化趋势,可以发现正畸模型组和低浓度尼古丁处理正畸模型组在14天达到改建的最大程度,并在此后转入修复期,而高浓度尼古丁处理正畸模型组则在21天时间点,牙槽骨依旧呈现出改建趋势。以上结果表明高浓度尼古丁涂抹给药可以明显加快大鼠正畸牙的牙周改建过程,并可延长改建过程。相对于其他类似实验^[20],本实验结果变化更为明显,其原因可能在于给药作用方式不同,口腔涂抹的尼古丁溶液可以被粘膜组织等充分吸收并直接作用于正畸牙及其附着组织,故造成的影响也较为明显。分子生物学检测结果显示 IL-17 水平及破骨细胞数量的变化趋势与 CT 检测指标所反映的牙槽骨改建过程一致,进一步验证了高浓度尼古丁涂抹给药可以明显加快大鼠正畸牙的牙周改建过程。

综上所述,高浓度尼古丁可以加快大鼠正畸牙的牙周改建过程,并可在一定程度上延长改建过程,这为正畸医师引导患者戒烟提供理论依据。低浓度尼古丁组对正畸改建影响不大,与单纯正畸的牙周改建接近,说明少量吸烟的患者也可以进行正畸治疗,该结论对于正畸治疗具有一定的临床指导意义。

参考文献(References)

- Hasegawa M, Adachi T, Takano-Yamamoto T. Computer simulation of orthodontic tooth movement using CT image-based voxel finite element models with the level set method [J]. Comput Methods Biomech Biomed Engin, 2016, 19(5): 474-483
- 陈翔, 周志斐, 刘芬, 等. 尼古丁对全身及口腔牙周组织的病理作用研究[J]. 现代生物医学进展, 2015, 15(9): 1778-1780
Chen Xiang, Zhou Zhi-fei, Liu Fen, et al. Study on the Deteriorating Effects of Nicotine Toward the Systematic and Periodontal Tissues[J].
- Progress in Modern Biomedicine, 2015, 15(9): 1778-1780
- Wu LZ, Duan DM, Liu YF, et al. Nicotine favors osteoclastogenesis in human periodontal ligament cells co-cultured with CD4 (+)T cells by upregulating IL-1β[J]. Int J Mol Med, 2013, 31(4): 938-942
- Xiong Q, Zhang L, Ge W, et al. The roles of interferons in osteoclasts and osteoclastogenesis[J]. JointBoneSpine, 2016, 83(3): 276-281
- Lee Y, Awasthi A, Yosef N, et al. Induction and molecular signature of pathogenic TH17 cells[J]. Nat Immunology, 2012, 13(10): 991-999
- 杨栋, 李红梅, 刘林花, 等. Th17 及其相关因子在不同牙周炎症状态龈沟液中的检测[J]. 口腔医学研究, 2017, 11(33): 1161-1164
Yang Dong, Li Hong-mei, Liu Lin-hua, et al. Detection of Th17 and Related Factors in Gingival Crevicular Fluid of Patients with Different Periodontal Inflammatory Status[J]. Journal of Oral Science Research, 2017, 11(33): 1161-1164
- 陈鹏, 杨风雪, 周建萍, 等 Micro-CT 动态观察大鼠牙齿移动过程中微观结构的变化 [J]. 上海交通大学学报(医学版), 2017, 37(2): 193-198
Chen Peng, Yang Feng-xue, Zhou Jian-ping, et al. Micro-structure changes in rat tooth movement process through micro-computed tomography dynamic observation [J]. Journal of Shanghai Jiao Tong University(Medical Science), 2017, 37(2): 193-198
- Tang L, Chen X, Bao Y, et al. CT Imaging Biomarkers of Bone Damage Induced by Environmental Level of Cadmium Exposure in Male Rats[J]. Biol Trace Elem Res, 2016, 170(1): 146-151
- Neldam CA, Lauridsen T, Back A, et al. Application of high resolution synchrotron micro-CT radiation in dental implant osseointegration[J]. J Craniomaxillofac Surg, 2015, 43(5): 682-687
- 郭妍芳, 陈岩. Micro-CT 及其在口腔正畸学中的应用 [J]. 疾病监测与控制杂志, 2014, 8(5): 298-300
Guo Yan-fang, Chen Yan. Principle and application of Micro-Computed Tomography in orthodontics [J]. Disease monitor & control, 2014, 8(5): 298-300
- Sood M, Bhatt P, Sessle BJ. Mechanical and thermal hypersensitivities associated with orthodontic tooth movement: a behavioral rat model for orthodontic tooth movement-induced pain [J]. J Oral Facial Pain Headache, 2015, 29(1): 60-69
- Xu Y, Zhao T, Xu W, et al. Periodontal microstructure change and tooth movement pattern under different force magnitudes in ovariectomized rats: an in-vivo microcomputed tomography study[J]. Am J Orthod Dentofacial Orthop, 2013, 143(6): 828-836
- Gonzalez-Garcia R, Monje F. Is micro-computed tomography reliable to determine the microstructure of the maxillary alveolar bone? [J]. Clin Oral Implants Res, 2013, 24(7): 730-737 (下转第 2441 页)

Lett, 2018, 414: 44-56

- [10] Ni Z, He J, Wu Y, et al. AKT-mediated phosphorylation of ATG4B impairs mitochondrial activity and enhances the Warburg effect in hepatocellular carcinoma cells[J]. *Autophagy*, 2017, 22: 1-43
- [11] Xiao Y, Peng H, Hong C, et al. PDGF Promotes the Warburg Effect in Pulmonary Arterial Smooth Muscle Cells via Activation of the PI3K/AKT/mTOR/HIF-1 α Signaling Pathway [J]. *Cell Physiol Biochem*, 2017, 42(4): 1603-1613
- [12] Shen Y, Liu Y, Sun T, et al. LincRNA-p21 knockdown enhances radiosensitivity of hypoxic tumor cells by reducing autophagy through HIF-1/Akt/mTOR/P70S6K pathway [J]. *Exp Cell Res*, 2017, 358(2): 188-198
- [13] Yuan LW, Yamashita H, Seto Y. Glucose metabolism in gastric cancer: The cutting-edge [J]. *World J Gastroenterol*, 2016, 22 (6): 2046-2059
- [14] Cai J, Niu X, Chen Y, et al. Emodin-induced generation of reactive oxygen species inhibits RhoA activation to sensitize gastric carcinoma cells to anoikis[J]. *Neoplasia*, 2008, 10(1): 41-51
- [15] Sun ZH, Bu P. Downregulation of phosphatase of regenerating liver-3 is involved in the inhibition of proliferation and apoptosis induced by emodin in the SGC-7901 human gastric carcinoma cell line [J]. *Exp Ther Med*, 2012, 3(6): 1077-1081
- [16] Zeng L, Zhou HY, Tang NN, et al. Wortmannin influences hypoxia-inducible factor-1 alpha expression and glycolysis in esophageal carcinoma cells[J]. *World J Gastroenterol*, 2016, 22(20): 4868-4880
- [17] Zhu Y, Ramos da Silva S, He M, et al. An Oncogenic Virus Promotes Cell Survival and Cellular Transformation by Suppressing Glycolysis [J]. *PLoS Pathog*, 2016, 12(5): e1005648
- [18] Lowry OH, Passonneau JV. The Relationships between Substrates and Enzymes of Glycolysis in Brain[J]. *J Biol Chem*, 1964, 239: 31-42
- [19] Nahm JH, Kim HM, Koo JS. Glycolysis-related protein expression in thyroid cancer[J]. *Tumour Biol*, 2017, 39(3): 1010428317695922
- [20] Mathupala SP, Ko YH, Pedersen PL. Hexokinase II: cancer's double-edged sword acting as both facilitator and gatekeeper of malignancy when bound to mitochondria[J]. *Oncogene*, 2006, 25: 4777-4786
- [21] Shoshan-Barmatz V, Zakar M, Rosenthal K, et al. Key regions of VDAC1 functioning in apoptosis induction and regulation by hexokinase[J]. *Biochim Biophys Acta*, 2009, 1787: 421-430
- [22] Liu X, Wang X, Zhang J, et al. Warburg effect revisited: an epigenetic link between glycolysis and gastric carcinogenesis [J]. *Oncogene*, 2010, 29(3): 442-450
- [23] Liu J, Pan C, Guo L, et al. A new mechanism of trastuzumab resistance in gastric cancer: MACC1 promotes the Warburg effect via activation of the PI3K/AKT signaling pathway [J]. *J Hematol Oncol*, 2016, 9(1): 76-82
- [24] Chen XS, Li LY, Guan YD, et al. Anticancer strategies based on the metabolic profile of tumor cells: therapeutic targeting of the Warburg effect[J]. *Acta Pharmacol Sin*, 2016, 37(8): 1013-1019
- [25] Phadngam S, Castiglioni A, Ferraresi A, et al. PTEN dephosphorylates AKT to prevent the expression of GLUT1 on plasmamembrane and to limit glucose consumption in cancer cells[J]. *Oncotarget*, 2016, 7(51): 84999-85020
- [26] Kitajima S, Lee KL, Hikasa H, et al. Hypoxia-inducible factor-1 α promotes cell survival during ammonia stress response in ovarian cancer stem-like cells[J]. *Oncotarget*, 2017, 8(70): 114481-114494
- [27] Hu L, Cui R, Liu H. Emodin and rhein decrease levels of hypoxia-inducible factor-1 α in human pancreatic cancer cells and attenuate cancer cachexia in athymic mice carrying these cells [J]. *Oncotarget*, 2017, 8(50): 88008-88020
- [28] Sui JQ, Xie KP, Zou W, et al. Emodin inhibits breast cancer cell proliferation through the ER α -MAPK/Akt-cyclin D1/Bcl-2 signaling pathway[J]. *Asian Pac J Cancer Prev*, 2014, 15(15): 6247-6251
- [29] Lin W, Zhong M, Yin H, et al. Emodin induces hepatocellular carcinoma cell apoptosis through MAPK and PI3K/AKT signaling pathways in vitro and in vivo[J]. *Oncol Rep*, 2016, 36(2): 961-967

(上接第 2451 页)

- [14] Ru N, Liu SS, Zhuang L, et al. In vivo microcomputed tomography evaluation of rat alveolar bone and root resorption during orthodontic tooth movement[J]. *Angle Orthod*, 2013, 83(3): 402-409
- [15] Papageorgiou SN, Kutschera E, Memmert S, et al. Effectiveness of early orthopaedic treatment with headgear: a systematic review and meta-analysis[J]. *Eur J Orthod*, 2017, 39(2): 176-187
- [16] Mizrak S, Turan V, Inan S, et al. Effect of nicotine on RANKL and OPG and bone mineral density[J]. *J Invest Surg*, 2014, 27(6): 327-331
- [17] Esfahrood ZR, Zamanian A, Torshabi M, et al. The effect of nicotine and cotinine on human gingival fibroblasts attachment to root surfaces [J]. *J Basic Clin Physiol Pharmacol*, 2015, 26(5): 517-522
- [18] Yang C, Zhang Y, Zhang Y, et al. Three-dimensional quantification of orthodontic root resorption with time-lapsed imaging of micro-computed tomography in a rodent model [J]. *J Xray Sci Technol*, 2015, 23(5): 617-626
- [19] An J, Li Y, Liu Z, et al. A micro-CT study of microstructure change of alveolar bone during orthodontic tooth movement under different force magnitudes in rats[J]. *Exp Ther Med*, 2017, 13(5): 1793-1798
- [20] Bakathir MA, Linjawi AI, Omar SS, et al. Effects of nicotine on bone during orthodontic tooth movement in male rats. Histological and immunohistochemical study[J]. *Saudi Med J*, 2016, 37(10): 1127-1135